Available online at www.sciencedirect.com
SCIENCE DIRECT®
Renewable and Sustainable Energy Reviews
11 (2007) 235–258
RENEWABLE & SUSTAINABLE ENERGY REVIEWS
www.elsevier.com/locate/rser

Flywheel energy and power storage systems

Björn Bolund*, Hans Bernhoff, Mats Leijon

Department of Engineering Sciences, Uppsala University, The Ångström Laboratory, Box 534, S-75121, Uppsala, Sweden

Received 20 December 2004; accepted 7 January 2005

Abstract

For ages flywheels have been used to achieve smooth operation of machines. The early models where purely mechanical consisting of only a stone wheel attached to an axle. Nowadays flywheels are complex constructions where energy is stored mechanically and transferred to and from the flywheel by an integrated motor/generator. The stone wheel has been replaced by a steel or composite rotor and magnetic bearings have been introduced. Today flywheels are used as supplementary UPS storage at several industries world over. Future applications span a wide range including electric vehicles, intermediate storage for renewable energy generation and direct grid applications from power quality issues to offering an alternative to strengthening transmission.

One of the key issues for viable flywheel construction is a high overall efficiency, hence a reduction of the total losses. By increasing the voltage, current losses are decreased and otherwise necessary transformer steps become redundant. So far flywheels over 10 kV have not been constructed, mainly due to isolation problems associated with high voltage, but also because of limitations in the power electronics. Recent progress in semi-conductor technology enables faster switching and lower costs. The predominant part of prior studies have been directed towards optimising mechanical issues whereas the electro technical part now seem to show great potential for improvement. An overview of flywheel technology and previous projects are presented and moreover a 200 kW flywheel using high voltage technology is simulated.

Keywords: High voltage generators; Generator; Motor; Generator simulation; Flywheel; Generator design; Energy storage

*Corresponding author. Tel.: +46 18 471 5817; fax: +46 18 471 5810.
E-mail address: bjorn.bolund@hvi.uu.se (B. Bolund).

1364-0321/$ - see front matter
doi:10.1016/j.rser.2005.01.004

Contents

1. Introduction . . . 236
2. Flywheel basics . . . 238
   2.1. Energy storage in flywheels . . . 238
   2.2. Magnetic bearings . . . 241
3. Flywheel technical considerations . . . 241
   3.1. Motor/generator . . . 241
   3.2. High voltage . . . 243
   3.3. Number of poles . . . 243
   3.4. Power electronics . . . 244
   3.5. Work done to date . . . 245
      3.5.1. Small-scale . . . 245
      3.5.2. Peak power buffers . . . 245
      3.5.3. Wind-diesel generator with a flywheel energy storage system . . . 245
      3.5.4. Flywheel for photovoltaic system . . . 246
      3.5.5. Harmonics . . . 246
      3.5.6. Flywheel in distribution network . . . 246
      3.5.7. High power UPS system . . . 246
      3.5.8. UPS system . . . 246
      3.5.9. Aerospace applications . . . 246
      3.5.10. High voltage stator . . . 246
      3.5.11. Of the shelf systems . . . 247
   3.6. Losses . . . 247
   3.7. External gyroscopic aspects . . . 249
   3.8. Safety . . . 249
4. Simulation of motor/generator . . . 249
   4.1. Mathematical model of the generator . . . 249
   4.2. Assumptions and design objectives . . . 251
   4.3. Motor/generator design . . . 252
5. Results from simulation . . . 253
6. Discussions . . . 255
7. Conclusions . . . 256
   Acknowledgements . . . 256
   References . . . 256

1. Introduction

Several hundred years ago pure mechanical flywheels where used solely to keep machines running smoothly from cycle to cycle, thereby render possible the industrial revolution. During that time several shapes and designs where implemented, but it took until the early 20th century before flywheel rotor shapes and rotational stress were thoroughly analysed [1]. Later in the 1970s flywheel energy storage was proposed as a primary objective for electric vehicles and stationary power backup. At the same time fibre composite rotors where built, and in the 1980s magnetic bearings started to appear [2]. Thus the potential for using flywheels as electric energy storage has long been established by extensive research.

More recent improvements in material, magnetic bearings and power electronics make flywheels a competitive choice for a number of energy storage applications. The progress in

power electronics, IGBTs and FETs, makes it possible to operate flywheel at high power, with a power electronics unit comparable in size to the flywheel itself or smaller. The use of composite materials enables high rotational velocity with power density greater than that of chemical batteries. Magnetic bearings offer very low friction enabling low internal losses during long-term storage. High speed is desirable since the energy stored is proportional to the square of the speed but only linearly proportional to the mass.

There are a number of attributes that make flywheels useful for applications where other storing units are now used.

- High power density.
- High energy density.
- No capacity degradation, the lifetime of the flywheel is almost independent of the depth of the discharge and discharge cycle. It can operate equally well on shallow and on deep discharges. Optimizing e.g. battery design for load variations is difficult.
- The state of charge can easily be measured, since it is given by the rotational velocity.
- No periodic maintenance is required.
- Short recharge time.
- Scalable technology and universal localization.
- Environmental friendly materials, low environmental impact.

One of the major advantages of flywheels is the ability to handle high power levels. This is a desirable quality in e.g. a vehicle, where a large peak power is necessary during acceleration and, if electrical breaks are used, a large amount of power is generated for a short while when breaking, which implies a more efficient use of energy, resulting in lower fuel consumption.

Individual flywheels are capable of storing up to 500 MJ and peak power ranges from kilowatts to gigawatts, with the higher powers aimed at pulsed power applications.

The fast responstime in flywheels makes them suitable to balance the grid frequency. As the energy contribution from more irregular renewable energy sources increases, this can be an important quality which will grow in importance [3].

The tools used for motor/generator design are also continuously improving to yield a more correct picture of the induction process. Powerful computer programs, where full electromagnetic field calculations are considered, have reduced a number of limitations and approximations at the design stage. Along with technical progress, especially regarding high voltage generators, each machine can be designed to match the physical conditions of the energy source and of the load. In this way the electric efficiency of new machines can be increased significantly.

High current yields substantial resistive power loss in the stator cables. To maximize the conductor area and thereby reduce the cable resistance, conventional generators use rectangular conductors. In theory it would be advantageous to build a generator that produces high voltage and low current, as the resistive power loss in the stator cables is proportional to the square of the current. Such a generator needs insulated circular conductors, for example conventional high voltage extruded solid dielectric cables [4]. This new class of generators is called Powerformer™ [5–8].

The aim of this article is to give an overview of flywheel technology, its applications and present development. Furthermore the possibility of using high voltage motor/generators

in flywheels are discussed and a generator constructed with XLPE- suited for flywheel mounting is simulated and data are presented.

2. Flywheel basics

2.1. Energy storage in flywheels

A flywheel stores energy in a rotating mass. Depending on the inertia and speed of the rotating mass, a given amount of kinetic energy is stored as rotational energy. The flywheel is placed inside a vacuum containment to eliminate friction-loss from the air and suspended by bearings for a stabile operation. Kinetic energy is transferred in and out of the flywheel with an electrical machine that can function either as a motor or generator depending on the load angle (phase angle). When acting as motor, electric energy supplied to the stator winding is converted to torque and applied to the rotor, causing it to spin faster and gain kinetic energy. In generator mode kinetic energy stored in the rotor applies a torque, which is converted to electric energy. Fig. 1 shows the basic layout of a flywheel energy storage system [9]. Apart from the flywheel additional power electronics is required to control the power in- and output, speed, frequency etc.

The kinetic energy stored in a flywheel is proportional to the mass and to the square of its rotational speed according to Eq. (1).

$$E_{\mathrm{k}} = \frac{1}{2}\boldsymbol{I}\omega^2 \tag{1}$$

where E_{k} is kinetic energy stored in the flywheel, $\boldsymbol{I}$ is moment of inertia and ω is the angular velocity of the flywheel. The moment of inertia for any object is a function of its shape and mass. For steel rotors the dominant shape is a solid cylinder giving the following expression for $\boldsymbol{I}$:

$$\mathbf{I} = \frac{1}{2}r^2 m = \frac{1}{2}r^4 \pi a \rho \tag{2}$$

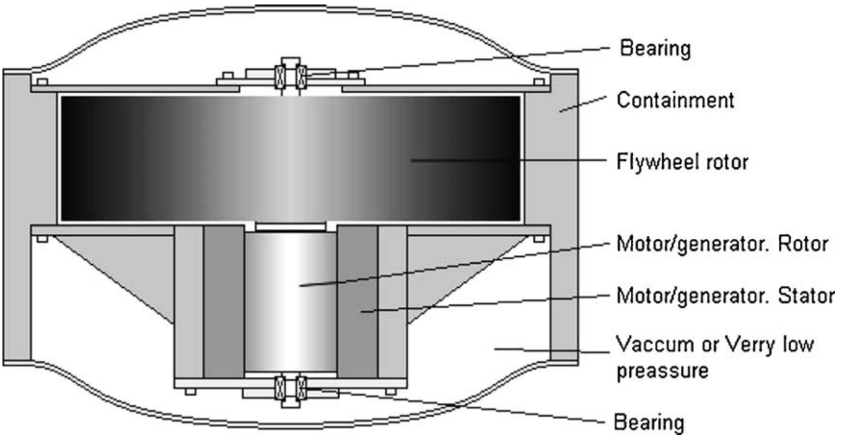


Fig. 1. Basic layout of a flywheel energy storage system [9].

where r is the radius and a is the length of the cylinder, m represents the mass of the cylinder and ρ is the density of the cylinder material. The other dominating shape is a hollow circular cylinder, approximating a composite or steel rim attached to a shaft with a web, which leads to Eq. (3).

$$\boldsymbol{I} = \frac{1}{4}m(r_0^2 + r_\mathrm{i}^2) = \frac{1}{4}\,\pi a\rho(r_0^4 - r_\mathrm{i}^4) \tag{3}$$

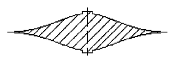
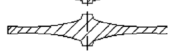
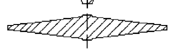
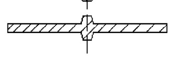
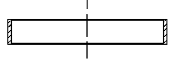
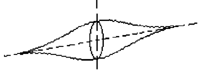
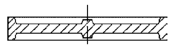
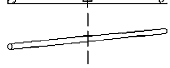
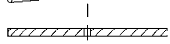
Eq. (1) shows that the most efficient way to increase the stored energy is to speed up the flywheel. The speed limit is set by the stress developed within the wheel due to inertial loads, called tensile strength σ. Lighter materials develop lower inertial loads at a given speed therefore composite materials, with low density and high tensile strength, is excellent for storing kinetic energy [10]. The maximum energy density with respect to volume and mass, respectively, is:

$$e_\mathrm{v} = K_\sigma \quad e_\mathrm{m} = K\sigma/\rho \tag{4}$$

where e_v and e_m is kinetic energy per unit volume or mass, respectively, K is the shapefactor, σ is maximum stress in the flywheel and ρ is mass density. In case of planar stress, if the height of the disk is small compared with the diameter, and a homogenous isotropic material with Poisson ratio of 0.3, i.e. steel, is used, the K factors are given in Table 1 [11].

In a three-dimensional object there will be three-dimensional interaction of material stresses. For a rotor constructed with a non-isotropic material, like fibre-reinforced composite, that stress interaction will limit the practical dimensions possible. Taking into account safety issues the resultant flywheel design is based on a hollow cylinder, in which material stresses created by three-dimensional effects are minimized. In short designs, the

Table 1
Shape-factor K for different planar stress geometries

Fly wheel geometry	Cross section	Shape factor **K**
Disc		1.000
Modified constant stress disc		0.931
Conical disc		0.806
Flat unpierced disc		0.606
Thin firm		0.500
Shaped bar		0.500
Rim with web		0.400
Single bar		0.333
Flat pierced bar		0.305

two stresses of primary concern are the radial stress and the hoop stress, Fig. 2. For an isotropic material the radial stress is expressed by Eq. (5).

$$\sigma_{\mathrm{r}} = \frac{3+v}{8}\,\rho\omega^2\left(r_0^2 + r_{\mathrm{i}}^2 - \frac{r_0^2 r_{\mathrm{i}}^2}{r^2} - r^2\right) \tag{5}$$

where ρ is the mass density, ω is the rotor speed, v represent the Poisson ratio r_0 is the outer radius of the rotor, r_{i} is the inner radius of the rotor and r represent any radius within the rotor.

The hoop stress is expressed by Eq. (6)

$$\sigma_{\theta} = \frac{3+v}{8}\,\rho\omega^2\left(r_0^2 + r_{\mathrm{i}}^2 + \frac{r_0^2 r_{\mathrm{i}}^2}{r^2} - \frac{1+3v}{3+v}\,r^2\right) \tag{6}$$

Table 2 presents characteristics for common rotor materials [12].

By making fiber reinforced composite rotors with circumferentially oriented fibers, the flywheel is more likely to develop circumferential cracks, which are much less likely to produce free-flying projectile fragments in case of a catastrophic failure. In most designs a rotational speed drop of 50% is allowed, thus the available energy is 75% of the stored energy, in other words the depth of discharge is 75%. Overall the flywheel geometry and speed determines the energy storage capability, whilst the motor/generator and power electronics determines the power capabilities.

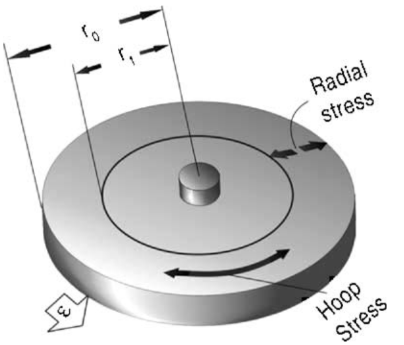


Fig. 2. Radial- and hoop stress in a short hollow cylinder rotating about its axis with angular velocity ω.

Table 2
Data for different rotor materials

Material	Density (kg/m^3)	Tensile strength (MPa)	Max energy density (for 1 kg)	Cost ($/kg)
Monolithic material 4340 Steel	7700	1520	0.19 MJ/kg = 0.05 kWh/kg	1
Composites				
E-glass	2000	100	0.05 MJ/kg = 0.014 kWh/kg	11.0
S2-glass	1920	1470	0.76 MJ/kg = 0.21 kWh/kg	24.6
Carbon T1000	1520	1950	1.28 MJ/kg = 0.35 kWh/kg	101.8
Carbon AS4C	1510	1650	1.1 MJ/kg = 0.30 kWh/kg	31.3

2.2. Magnetic bearings

Mechanical bearings used in the past cannot, due to the high friction and short life, be adapted to modern high-speed flywheels. Instead a permanent or electro permanent magnetic bearing system is utilized. Electro permanent magnetic bearings do not have any contact with the shaft, has no moving parts, experience little wear and require no lubrication. It consists of permanent magnets, which support the weight of the flywheel by repelling forces, and electromagnets are used to stabilize the flywheel, although it requires a complex guiding system. An easier way to stabilize is to use mechanical bearings at the end of the flywheel axle, possible since the permanent magnet levitates the flywheel and, thus, reduce the friction [13,14]. The best performing bearing is the high-temperature super-conducting (HTS) magnetic bearing, which can situate the flywheel automatically without need of electricity or positioning control system. However, HTS magnets require cryogenic cooling by liquid nitrogen [12].

3. Flywheel technical considerations

For decades, most engineers have used the concept of storing kinetic energy in a spinning mass to smooth their operation. Until recently the vast majority constituted of steel wheels coupled with a motor/generator, where the high rotary inertia allowed long ride-through time without significant decrease in flywheel rotational speed. Since the change in rotational speed directly reflects the electrical frequency the power delivery of those flywheels rarely exceeded 5% of the stored energy.

3.1. Motor/generator

Requirements for standardized electric power have made most flywheel system designers elect variable speed AC generators (to accommodate the gradual slowing of the flywheel during discharge) and diodes to deliver DC electricity. The two major types of machines used are the axial-flux- and the radial-flux permanent magnet machines (AFPM and RFPM, respectively). There are numerous alternatives for the design of an AFPM machine such as internal rotor, internal stator, multidisc, slotted or slot-less stator, rotors with interior or surface-mounted magnets [15–18]. Unlike radial machines, axial machines can have two working surfaces. Either two rotors combined with one stator or one rotor combined with two stators. The benefit of using a two surface working machine is the increase in power output [17,19]. The axial machines seem to have more advantages over the radial such as, a planar adjustable air gap and easy cooling arrangements, which is important when working under low-pressure conditions [20]. Fig. 3a shows a one-rotor two stator AFPM configuration without the cable winding in the stators. It can be seen that the permanent magnets are an integral part of the flywheel rotor and the stators are fixed to the housing.

A permanent-magnet axial-flux motor, resembling the 200 kW motor/generator simulated later in this article, is analysed by Furlani [21]. An analytical expression for a two dimensional field solution of the magnetic field is presented for a simple pole structure. The permeability for the magnetic field return path is set to infinity.

Much attention has been directed towards optimising radial gap machines [22–24]. In a RFPM machine the magnets can be surface mounted on the rotor axle surrounded by the

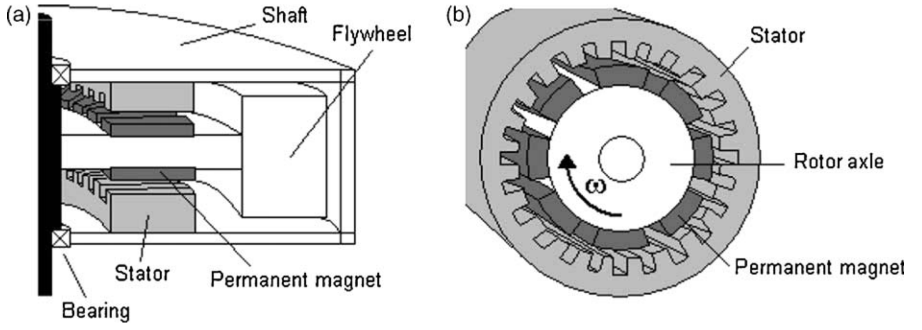


Fig. 3. (a) show an AFPM machine arrangement and (b) show an RFPM machine arrangement.

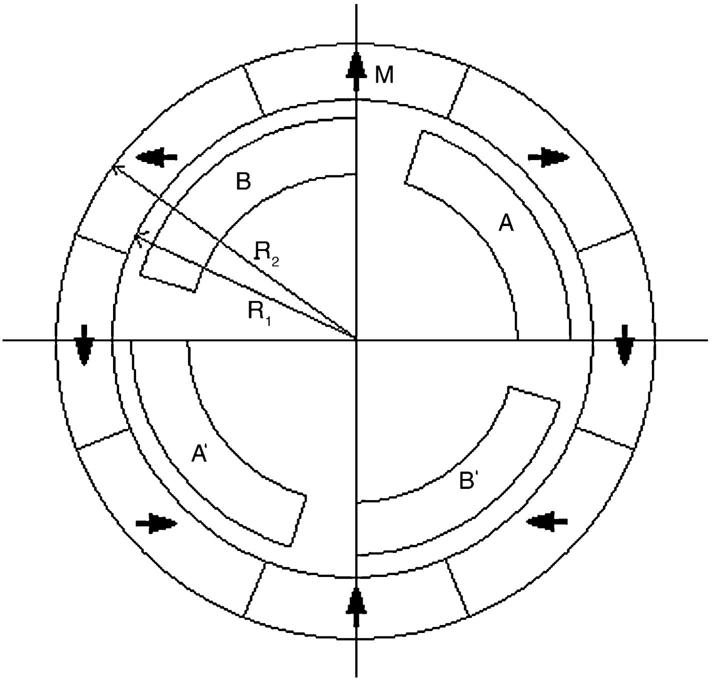


Fig. 4. Cross section of internal dipole array for $n = 8$.

stator, as in Fig. 3b, or mounted in a ring enclosing the stator. The radial flux machine is mostly used in small-scale high-speed machines, where the tensile strength of the permanent magnets demands placing close to the rotating axle.

Another type of motor/generator is the internal-dipole, Halbach-type magnet arrays. Where the PM array rotates with the flywheel and interacts with a set of stationary coils to produce torque. In a Halbach array, n PM segments forming a cylindrical shell about an axis create the internal dipole. A cross section of an internal dipole array with 8 segments, where M is the magnetization is shown in Fig. 4, inside a single turn two-phase stator is

also shown. The Halbach type motor can also be of multi-pole type. One of the advantages of this configuration is the low external magnetic field produced when a steel rim is placed outside the magnets. Within the shell a dipole configuration creates a uniform flux B [25].

$$B = B_{\text{rem}} \log\left[\frac{r_2}{r_1}\right]\kappa \tag{7}$$

$$\kappa = \frac{\sin\left(\frac{2\pi}{p}\right)}{\frac{2\pi}{p}} \tag{8}$$

where B is the resultant uniform flux, B_{rem} is the remanent flux in permanent magnets, r_2 equals outer radius and r_1 equals inner radius and p is the number of poles.

The torque generated is then proportional to the ampere turns and radius from the rotational center [25].

$$T = Bilr \tag{9}$$

where T equals torque, B is the magnetic flux, l is the length of the conductor, i is the current and r equals the radius.

Machines with operating voltage in the range of 70–400 V have been built [26,27].

3.2. High voltage

Even though different kinds of flywheels constructed today benefit from the recent progress in technology, there is one thing all of them have in common, the inability to directly produce high voltage (>36 kV). So-called 'high voltage' flywheels have been constructed. However, the highest voltage attained so far is a 10-pole permanent magnet machine with a continuous voltage of 6.7 kV and a peak voltage of 10 kV constructed in 2001 [28]. The result is that for true high voltage applications a transformer has to be used, introducing more unwanted losses.

Apart from the PM motor/generator used in almost all flywheels there is also the possibility of using a Synchronous Reluctance Motor/Generator. In 1996 a 60 kW flywheel, utilizing this motor, was developed [29]. Table 3 shows advantages/disadvantages with PM and induction machines.

3.3. Number of poles

The choice of number of poles to be used in a machine is essential to the overall performance. Two pole motor/generators are most common in high-speed machines, mainly to keep the voltage down but it also has other good properties. Depending on axialor radial flux configuration a multi-pole rotor can experience substantial electromagnetic axial or radial forces generated by the stator winding, if there is a net attractive force between a pole-pair and the stator. In a two-pole rotor, however, the only two poles are directly opposite one another resulting in a net force on the rotor of approximately zero. Eliminating these forces reduces the load requirements on the bearings, which is particularly important if magnetic bearings are used.

Table 3
Advantages and disadvantages with PM and induction machines

	High voltage PM machine	PM machine	Induction machine
Advantages	+ High overload capability, due to low load angle and low stator current	+ Magnetic field is produced without excitation losses	+ No concern with demagnetization
	+ Magnetic field is produced without excitation losses	+ Less complex rotor design, no need of electric wires in the rotor	+ No excitation field at zero torque, hence no electromagnetic spinning losses
	+ Less complex rotor design, no need of electric wires in the rotor	+ Possible to achieve a higher overall efficiency	+ Can be constructed from high-strength low-cost materials
	+ Possible to achieve a higher overall efficiency		
Disadvantages	− Risk of demagnetization and a decreasing intrinsic coercivity with increasing temperature	− Risk of demagnetization and a decreasing intrinsic coercivity with increasing temperature	− RI^2, transformer and rectifying losses in the electromagnets during field excitation
	− Machines with iron in the stator experience electromagnetic spinning losses at zero-torque	− Machines with iron in the stator experience electromagnetic spinning losses at zero-torque	− More complex rotor design, due to the need of wires and electric brushconnection to the rotor
	− The low tensile strength of PM materials require structural support against centrifugal forces, leaving constraints on the design of high-speed, high-power rotors	− The low tensile strength of PM materials require structural support against centrifugal forces, leaving constraints on the design of high-speed, high-power rotors	− Rotor brushes require maintenance
			− Poor overload capability due to the high stator current

3.4. Power electronics

A brushless permanent magnet generator (in a flywheel) produces variable frequency AC current. In most applications though, the load requires a constant frequency making it necessary to first rectify the current and then convert it back to AC. Power converters for energy storage systems are based on SCR, GTO or IGBT switches. In an early stage of energy storage utility development, SCRs where the most mature and least expensive semiconductor suitable for power conversion. SCRs can handle voltages up to 5 kV, currents up to 3000 A and switching frequencies up to 500 Hz. Due to the need of an energized power line to provide the external on/off signal to those switches they where replaced with GTOs, which do not depend on an energized line to function. The GTO device can handle voltages up to 6 kV, currents up to 2000 A and switching frequencies up to 1 kHz. In the last several years IGBTs has emerged, Fig. 5. The IGBT is a solid-state switch device with ability to handle voltages up to 6.7 kV, currents up to 1.2 kA and most important high switching frequencies [30,31].

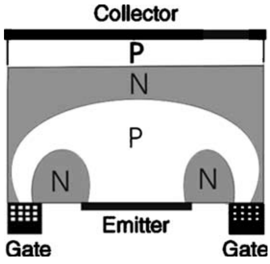


Fig. 5. IGBT schematic.

The technique used to produce AC current from DC is called Pulse-Width Modulation (PWM). Pulses of different length are applied to the IGBTs in the inverter, causing the DC current to be delayed by the inductive load and a sine wave is modulated [32]. A fast switching frequency in the power converter improves emulation of a sine wave mainly by eliminating some of the higher order harmonics. To reduce the harmonic content even further a filter, consisting of capacitors and inductors can be connected on the AC side of the output.

Electromechanical energy conversion systems have been explored in order to make them more fault-tolerant [33]. By using three single-phase inverters instead of one compact setup a more flexible design is achieved along with advantages like the ability to operate even in the event of a single-phase fault.

3.5. Work done to date

3.5.1. Small-scale

Small-scale flywheel energy storage systems have relatively low specific energy figures once volume and weight of containment is comprised. But the high specific power possible, constrained only by the electrical machine and the power converter interface, makes this technology more suited for buffer storage applications. Development of alternative dual power source electric vehicle systems that combine a flywheel peak power buffer with a battery energy source has been undertaken [18,34].

3.5.2. Peak power buffers

The uses of a flywheel as power buffer in an electric vehicle can significantly reduce the peak currents drawn from the ordinary storing supply e.g. battery. Elimination of the peak currents will prolong the battery life [34].

3.5.3. Wind-diesel generator with a flywheel energy storage system

In the year 2000 a simulation of a Wind-Diesel generation plant together with a kinetic energy storage unit was presented and the construction of it was undertaken. The goal of this system is a unit where the regular wind oscillations are compensated by the diesel generator and the flywheel. The 0.6 kWh, 50 kW flywheel is able to supply active and reactive power to compensate both frequency and voltage of the network. The unit is designed to supply total power during a period of 1.8 min with a rated voltage 750 V and a maximum current of 102 A [35].

3.5.4. Flywheel for photovoltaic system

A doubly salient permanent magnet (DSPM) motor flywheel energy storage for building integrated photovoltaic (BIPV) system was simulated in 2001. By adding a flywheel to a BIPV equipped building situated in Hong Kong, the load supply time can be prolonged from 9 a.m. to 3 p.m. to 8 a.m.-beyond 6 p.m. [36].

3.5.5. Harmonics

Different flywheel systems for compensating harmonics in low voltage (~400 V) power networks have been compared and analysed. Up to the eleventh harmonic a decrease of about 50% was accomplished [37].

3.5.6. Flywheel in distribution network

A 10 MJ flywheel energy storage system, used to maintain high quality electric power and guarantee a reliable power supply from the distribution network, was tested in the year 2000. The FES was able to keep the voltage in the distribution network within 98–102% and had the capability of supplying 10 kW of power for 15 min [38].

3.5.7. High power UPS system

A 50 MW/650 MJ storage, based on 25 industry established flywheels, was investigated in 2001. Possible applications are energy supply for plasma experiments, accelerations of heavy masses (aircraft catapults on aircraft carriers, pre-acceleration of spacecraft) and large UPS systems. The 50 MW peak power can be supplied for about 13 s, with an overall efficiency of 91–95%. The flywheels are connected in parallel to a 1200 V DC-link. Similar PM flywheels have previously been tested in urban traffic busses and rail systems with a resulting energy save of up to 40% [39].

3.5.8. UPS system

A Case study on an existing medium voltage network has been carried out, in which different disturbance scenarios have been simulated (voltage dips, start-up etc). The idea was to connect four 1.6 MVA flywheel based dynamic UPS systems combined with a diesel generator to the 20 kV distribution network, thereby improving the power quality. The simulation results indicate that the approach is feasible, and show a significant improvement in power quality. Typically, the voltage dips is divided by a factor 3 even in the worst cases. A transformer is required between the flywheel storage system and the medium voltage network [40].

3.5.9. Aerospace applications

A two pole, three-phase PM synchronous motor/generator coupled to a flywheel have been simulated. The flywheel storage unit is intended to replace a battery storage unit onboard the International Space Station. The motor is rated to 7 kVA, 80 V and 50 A and 1000 Hz. A comparison between flywheel and NiH_2 battery systems for an EOS-AMI type spacecraft has shown that a flywheel system would be 35% lighter and 55% smaller in volume [41].

3.5.10. High voltage stator

A 10 pole PM machine with a continuous voltage of 6.7 kV and peak voltage of 10 kV was constructed in 2001, for use in hybrid electric combat systems. The 25 MJ flywheel is to

produce a continuous power of 350 kW (loss 2.4 kW) as well as intermittent 5 MW pulses, the idling loss is calculated to be around 250 W. To handle the heat produced, the stator is cooled by 70 or 90 °C oil. The insulation on the cables constitute of filler epoxy (type 1) and FEP tubes surrounded by epoxy (type 2) see Fig. 6. The overall size and weight of the system is 0.28 m^3 and 519 kg [28].

3.5.11. *Of the shelf systems*

The operating voltages of three available flywheel systems from different companies can be found in Table 4.

3.6. *Losses*

The integrated motor/generator is usually of a rotating-field deign, where the field is supplied either by electromagnets or by rare-earth permanent magnets. The properties of high field permanent magnets yield flux densities high enough to enable machines with slotless armature windings, also known as air-gap windings, without a magnetic stator core [42]. Absence of a ferromagnetic material in the stator has two major impacts on the performance of a motor/generator. First of all the low permeability will quickly reduce the magnetic field strength when moving away from the magnet. As a result the induced voltage becomes lower, thus also diminishing the generated power. Second, there will not be any heat loss in the stator core due to hysteresis effects. The hysteresis loss is otherwise

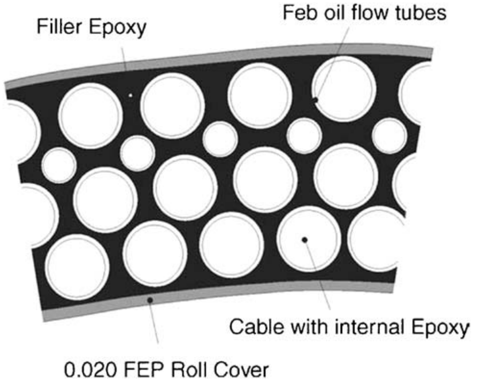


Fig. 6. Cross section of the 6.7 kV Stator [28].

Table 4
Operating voltage of three different flywheel systems [12]

Developed by:	Type	Power (kW)	Voltage (V)
EMAFER	Medium power	300	<1000
Magnet motor	Medium power	150	300–800
Magnet motor	High power	5000	—
URENCO	Medium power	100	600–750

always present when exposing a ferromagnetic material to magnetic flux [43]. It is clear that higher frequencies convey more losses and that hysteresis loss in the stator core will have severe impact during long time (stand-by) energy storage in a flywheel. Without hysteresis loss the stand-by losses are very small and limited to those of leak eddy currents and bearing losses.

The low tensile strength of the magnets compared to that of the composite flywheel limits their placing to the vicinity of the hub. As a consequence the number of poles, and therefore the rate of change of magnetic flux, must be carefully selected in order to achieve the desired voltage. Table 5 shows the tensile strength for common magnetic materials [44].

Traditionally used ferrites do not, due to their low conductivity, give rise to induced eddy currents on the surface. Some of the sintered rare earth materials, however, have large conductivity and therefore suffer from such problems. Eddy currents on the surface of the magnets arise when the magnetic field from the stator interacts with the magnets and are roughly:

$$J_{\text{magnet}} = \frac{\sigma}{l_{\text{magnet}}} \frac{\mathrm{d}\Phi_{\text{stator}}}{\mathrm{d}t} \tag{10}$$

where J_{magnet} is the surface current density on the magnet, σ is the conductivity of the magnet, l_{magnet} is the length of the magnet, and Φ_{stator} is the magnetic flux from the stator. Since the magnetic flux form the stator is proportional to the current going through the stator windings and eddy current losses are squarely dependent on frequency, it is necessary to minimize the current harmonics.

A great deal of the total losses from the motor is ohmic (I^2R) losses in the stator winding. It is clear that those can be diminished either by increasing the amount of conducting material (usually copper), thereby decreasing the resistance, or by decreasing the current in the stator. There are obvious drawbacks associated with increasing the amount of conducting material such as increasing weight, cost and space. Induced high frequency eddy currents in the stator may also increase depending on the configuration. Decreasing the current in the stator inevitably leads to higher voltage if the overall power is to be maintained. So far it has been impossible to increase the voltage due to the risk of an electric breakdown, but if a higher voltage can be handled the copper losses can be decreased.

Table 5
Data for different magnetic materials [44]

Material	Density (kg/m^3)	Tensile strength (MPa)	Remanence (T)
Sintered Neodymium–Iron–Boron (Nd–Fe–B)	7400–7600	80	1.08–1.36
Sintered Samarium-Cobalt	8000–8500	60	0.75–1.2
Sintered Ferrite	4800–5000	9	0.2–0.43
Injection molded composite (Nd–Fe–B)	4200–5630	35–59	0.40–0.67
Compression molded composite (Nd–Fe–B)	6000	40	0.63–0.69
Injection molded composite Ferrite	2420–3840	39–78	0.07–0.30

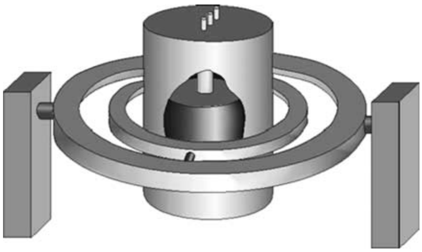


Fig. 7. Simple illustration of how to mount a flywheel in a vehicle for minimizing the effect of gyroscopic torques.

3.7. External gyroscopic aspects

For flywheels situated in a vehicle, satellite or space station the gyroscopic forces are important. In a satellite it is possible to make use of the gyroscopic force from a flywheel by letting it provide torque to the spacecraft for altitude control, thereby diminish the overall weight and increase the effective use of energy. In space stations and vehicles the flywheel batteries are controlled as pairs and situated to rotate in opposite direction to not produce any net torque [45,46]. Another way to cope with the interaction of gyroscopic forces in a vehicle when using just one flywheel is to place the flywheel in a gimbal system, thereby eliminating most of the gyroscopic torque. The gimbal system works in the same way as a cup-holder does in a vehicle, which means that the vehicle can turn and lean without tilting and twisting the position of the flywheel [47]. Fig. 7 shows a simplified picture of the gimbal system.

3.8. Safety

Some sort of inertial containment system becomes necessary to minimize the collateral damage from a failed flywheel. Reasons for failure could be, crack growth from material flaws created during manufacture, bearing failure or external shock loads. For large flywheels the vacuum chamber acts as a first safety enclosure in a multiple-barrier containment system to prevent rotor debris from flying free. The next barrier system design can include thick steel, concrete chambers and/or underground vaults. Small portable flywheels cannot utilize bulky containments like an underground vault. Instead the rotor is designed to fail safely (described above) in which case a vacuum vessel provides sufficient protection. It is also possible to simply place the FES units in restricted areas similar to what is done with conventional turbines that operates in electric power plants. Most machines have a vertical rotation axle, but horizontal machines also occur [48]. A vertical axle minimizes the possibility of mass centre displacement witch can lead to instabilities and damage the flywheel.

4. Simulation of motor/generator

4.1. Mathematical model of the generator

When a generator is simulated a two-dimensional model of the generator cross-section geometry is created. The geometry is based on straight lines and circular arcs. The

geometric domains are assigned a material with corresponding material properties such as resistivity, permeability, coercivity, sheet thickness, price etc. Voltage, current and thermal sources are given as scalars or by circuit equations.

A two-dimensional finite element method (FEM) is used in the calculations. To ensure high accuracy and fast computations the mesh is made more detailed in the air-gap and in the stator teeth and coarser in the yoke and the rotor rim. The accuracy can be set to different levels. To account for three-dimensional effects, coil-end reactances and resistances are calculated.

When calculating the induction in the stator the displacement current, $\partial \boldsymbol{D}/\partial t$, can, due to its long wavelength, be neglected. The displacement current is also directed in radial direction in the insulating dielectric material surrounding the stator cables and will thereby not contribute to any induction.

Without the displacement current Ampere's law can be written as:

$$\nabla \times \boldsymbol{H} = \boldsymbol{j} \tag{11}$$

where $\boldsymbol{H}$ is the magnetizing field and $\boldsymbol{j}$ represent the free current density. Material behaviour is described by Eqs. (12) and (13).

$$\boldsymbol{B} = \mu_{\mathrm{r}}\mu_0 \boldsymbol{H} \tag{12}$$

where $\mu_{\mathrm{r}}\mu_0$ is the magnetic permeability and $\boldsymbol{B}$ is the magnetic flux, Ohm's law,

$$\boldsymbol{j} = \sigma \boldsymbol{E} \tag{13}$$

where σ is the conductivity and $\boldsymbol{E}$ is the electric field. The $\boldsymbol{B}$-field can be expressed by the vector potential, $\boldsymbol{A}$, as:

$$\boldsymbol{B} = \nabla \times \boldsymbol{A} \tag{14}$$

Combining Eqs. (11)–(14) gives:

$$\nabla \times \left(\frac{1}{\mu_{\mathrm{r}}\mu_0} \nabla \times \boldsymbol{A} \right) = \sigma \boldsymbol{E} \tag{15}$$

Faradays law:

$$\nabla \times \boldsymbol{E} = -\frac{\partial \boldsymbol{B}}{\partial t} \tag{16}$$

in combination with Eq. (14) and Helmholtz' theorem gives:

$$\boldsymbol{E} = -\frac{\partial \boldsymbol{A}}{\partial t} - \nabla V \tag{17}$$

where V is the scalar potential. The two-dimensional nature of the model enables the vector potential to be expressed as:

$$\boldsymbol{A} = A_{\mathrm{z}}(r, \varphi, t)\hat{z} \tag{18}$$

which together with Eqs. (15) and (17) results in:

$$\sigma \frac{\partial A_z}{\partial t} = \nabla \cdot \left(\frac{1}{\mu_{\mathrm{r}}\mu_0} \nabla A_{\mathrm{z}} \right) - \sigma \frac{\partial V}{\partial z} \tag{19}$$

The term $\partial V/\partial z$ is traditionally called applied potential and can be given as an inparameter corresponding to a current density in z-direction. The time derivative of the vector potential in Eq. (19) is related to the penetration of a magnetic field in a material,

also called the skin effect. The skin depth in a material, δ_{skin}, is given by:

$$\delta_{\mathrm{skin}} \approx \frac{1}{\sqrt{\mu_{\mathrm{r}}\mu_0\sigma f}} \tag{20}$$

where f is the electric frequency of the generator.

A current source representation of Eq. (15) can be written as

$$\boldsymbol{\nabla} \times \frac{1}{\mu}\boldsymbol{\nabla} \times \boldsymbol{A} = \boldsymbol{J} + \boldsymbol{J}_{\mathrm{m}} \tag{21}$$

where $\boldsymbol{J}$ is the source current density given by Eq. (11) and the current density $\boldsymbol{J}_{\mathrm{m}}$ is given by Eq. (23) [49]. In the simulation tool Eq. (21) is solved for a number of different discrete rotor positions under transient conditions, where the distance between those positions is given by the rotor speed. The rotor and stator are connected with varying boundary conditions. Symmetries in both geometry and electromagnetic field enables the generator to be presented by a two dimensional unit-cell with periodical boundary conditions. Depending on the stator slot pitch the unit cell can include one or more rotor poles. In the case of a permanently magnetized rotor, as in this case the length of the permanent magnet is determined by iteration to give a sufficient induction.

Permanent magnets are modelled by a surface current density, $\boldsymbol{J}_{\mathrm{m,s}}$, determined by:

$$\boldsymbol{J}_{\mathrm{m,s}} = \hat{n} \times \boldsymbol{M} \tag{22}$$

where $\boldsymbol{M}$ is the magnetization.

If stator steel is used there will be distributions of non-linear magnetization and current in the stator. In that case the magnetization current, $\boldsymbol{J}_{\mathrm{m}}$, in the volume representing the stator steel is given by:

$$\boldsymbol{J}_{\mathrm{m}} = \boldsymbol{\nabla} \times \boldsymbol{M} \tag{23}$$

The Flywheel motor/generator simulated in this article uses no stator steel and therefore no attention needs to be paid to non-linear currents and magnetization in the stator. Thermal distribution in the generator is determined by Fick's law and the continuity equation for heat:

$$k\boldsymbol{\nabla}^2 T - \frac{\partial T}{\partial t} = -\boldsymbol{J}_{\mathrm{heat}} \tag{24}$$

where k is the diffusion coefficient and $\boldsymbol{J}_{\mathrm{heat}}$ is a heat source i.e. ohmic current losses, magnetic losses and external cooling. In addition to the field equations appropriate initial, boundary and jump conditions should be added. The values in the magnetization curves, BH-curves, for all materials have been experimentally derived by the Epstein method.

Electromagnetic losses in the generator consist mainly of ohmic and eddy current losses in the stator copper winding. The mesh in the FEM-solver has higher mesh density in areas of special interest such as in the air gap and in the stator. Among the calculation results are magnetic field plots, temperature distributions, iron and copper losses, load angles and reactances.

4.2. Assumptions and design objectives

A 200 kW three-phase PM generator intended for use in a flywheel storage unit, situated in for example a bus, has been simulated. To minimize stand-by losses an ironless stator

was preferred. To achieve high power density in a generator with an ironless stator, an axial flux topology where the stator cables are situated between one magnet and one ferromagnetic steel rim was chosen. The magnets used are of neodymium–iron–boron, NdFeB, type. As this material is conductive it is necessary to limit the current harmonics from the stator. Otherwise induced surface eddy currents in the magnets will cause excessive loss and heat development, which could deteriorate magnet characteristics. Conventional high voltage extruded solid dielectric cables are used for winding the stator [4].

Models for the electric circuit are added to the electromagnetic and thermal field equations. The equations describing the stator (armature) circuit are,

$$
\begin{aligned}
& i_a + i_b + i_c = 0 \\
& u_a + R_s i_a + L_s^{\text{end}} \frac{\partial i_a}{\partial t} - u_b - R_s i_b - L_s^{\text{end}} \frac{\partial i_b}{\partial t} = V_{ab} \\
& u_c + R_s i_c + L_s^{\text{end}} \frac{\partial i_c}{\partial t} - u_b - R_s i_b - L_s^{\text{end}} \frac{\partial i_b}{\partial t} = V_{cb}
\end{aligned} \tag{25}
$$

where u_a, u_b are the phase voltages, i_a, i_b are the phase currents, L_s^{end} is the coil end reactance (obtained from an separate three dimensional computation), and V_{ab}, V_{cb} are the line voltages of the external load circuit. The external load may be determined in more detail, by for instance including equations for rectifiers. However, a simple circuit with a resistive load is simulated here.

The internal (phase currents, phase voltages, rotor and stator equations) and the external (outer load) circuit equations are added to the system. Sources are described by circuit equations. A symmetric three-phase winding of the stator is modeled. The phases are mutually separated by $2\pi/3$ electrical radians. The main advantage of a symmetric threephase system is that the output power is only slowly varying with time (i.e. the variation of rotation speed) provided a proper design is made for the generator.

4.3. Motor/generator design

An air-wound axial flux machine is modeled. The upper rim rotates with the same speed as the magnet and the lower rim. Fig. 8 shows a cross-section of one pole.

Table 6 gives the properties of the generator.

The machine is studied for a rotational speed of 8000 rpm which corresponds to a tipspeed of 420 m/s for a carbon composite rotor with a diameter of 1 m. The machine has 12 poles and is designed to fit inside the carbon composite cylindrical rotor.

For simplicity the power factor $\cos\phi$ is chosen to 1 in the simulations (in a traditional rotating machine it is typically around 0.8). In a real construction, the power factor could be optimized to the predominant rotational frequency. However, if the machine is designed to work at low load angle, as in this case, the power factor will be close to unity for the entire operating range.

No assumption on the size or genometry of the carbon composite rotor, other than rotational frequency, are made. The machine is assumed to operate with a rotor that can store in the range of 5 kWh which in practice would correspond to a rotor mass of 30 kg.

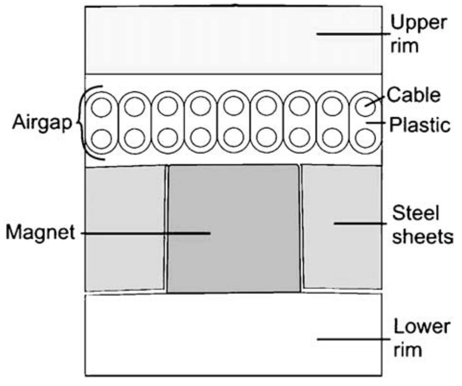


Fig. 8. Cross-section view of one generator pole.

Table 6
Generator properties

Power	200 kW
Voltage	1 kV
Current	115.5 A
Power factor, cos ϕ	1
Load angle	4.3°
Outer diameter	0.689 m
Rpm	8000
Max electric freq	800 Hz

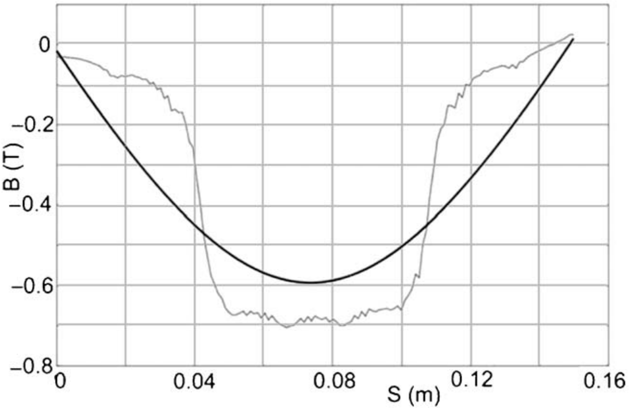


Fig. 9. Magnetic field in the air-gap for one pole. The grey line shows the B-field along a line in the middle of the air-gap and the black line is the fundamental of B.

5. Results from simulation

A plot of the magnetic field distribution along a line in the middle of the air-gap is shown in Fig. 9. The ripple causes a rapidly varying electromagnetic field on the rotor. This ripple

can cause vibration but also induce eddy currents which will contribute to losses as discussed above. Fluctuations can also be observed in the voltage output, Fig. 10.

A total amount of 4.9 dm^3 of magnets are used. Fig. 11 shows the magnetic field in the generator under load condition. The losses are given in Table 7 and the voltage harmonics produced are given in Table 8.

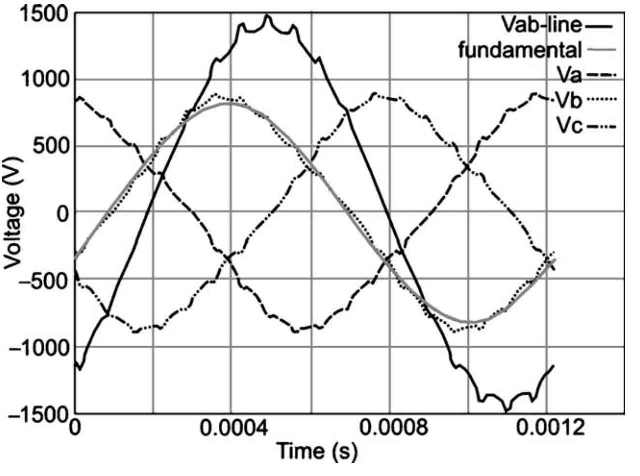


Fig. 10. Stator voltage output from the three phases in generating mode at full load.

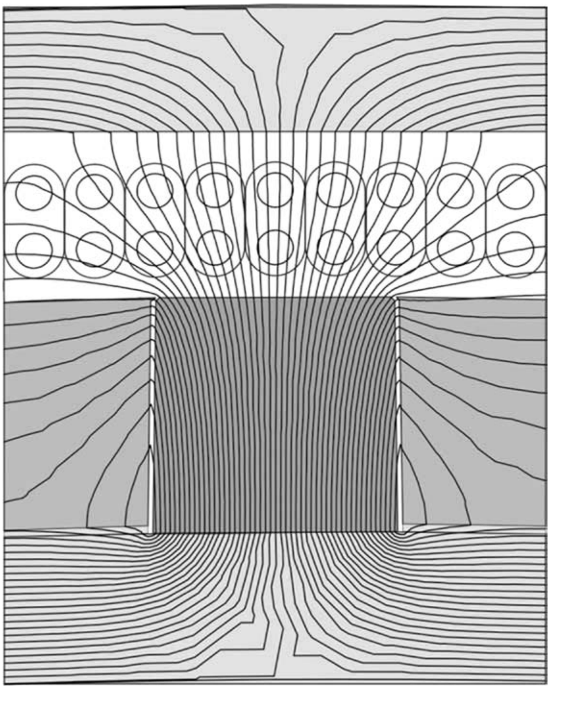


Fig. 11. Magnetic field distribution under full load in generator mode.

Table 7
Electric losses in the generator

Losses (kW)	
Ohmic copper loss in core	0.1
Ohmic end winding loss	0.29
Eddy current loss in windings	0.79

Table 8
Voltage harmonics in the stator

Phase harmonic	I (%)
1	100
3	6.8
5	0.4
15	1.0
17	1.9
19	1.7
21	0.6
33	0.4

The thermal computations are not yet complete, as some thermal insulation material properties outside the stator are not included. However, the maximum temperature of the generator is so far below 60° in all simulations. The increase in thermal load due to the low air-pressure around the motor/generator will be compensated by a water or air cooling system. A well-designed generator with low operational temperature opens for large overload capacities without operational worry of fast insulation degradation. The conductor area has been chosen to 16 mm^2, which is sufficient to avoid strong Ohmic heating.

6. Discussions

The calculations are based on a two-dimensional electromagnetic and thermal field model. Three-dimensional effects are not fully taken into account, but the coil-end reactance is included. The generator physics is described by field equations, and a conventional simplified circuit description ('equivalent circuit') is thus not the basis for the simulations.

One of the key issues for a working flywheel is to keep the induced eddy-currents to a minimum. Temperature rise in the rotor magnets due to eddy-currents from the phase harmonics needs to be analyzed. Different stator layouts will give rise to different amounts of harmonics, it is therefore crucial to simultaneously analyze eddy-currents and cooling. Although simulations show that the configuration used in the simulations work, there is still the need of simultaneous analyzing of the induced eddy-currents in the magnets as well as the need for experimental validation of the results.

The voltage harmonics listed in Table 8 can be observed as the voltage ripple in Fig. 10. The stator current will contain about the same harmonics and since the induced eddy

currents in the rotor magnets will depend strongly on the shape of that stator current, it is necessary to try to minimize harmonics.

For motor/generators operating under a low surrounding air-pressure, a high electric efficiency is crucial to avoid overheating. A high voltage ensures low currents which leads to low losses and opens for a large overload capability, up to 500 kW for this motor/generator. The stator winding arrangement and rotor pole shape will have large influence on the overall performance. A very interesting choice is to have magnets mounted at both sides of the stator, which would strongly enhance the magnetic field in the air-gap.

7. Conclusions

Flywheel storage systems have been used for a long time. Material and semiconductor development are offering new possibilities and applications previously impossible for flywheels. The fast rotation of flywheel rotors is suitable for direct generation of high voltage. Thus for flywheel applications, the motor/generator part has a large upgrade potential. In this article a 200 kW permanent magnet air gap winding motor/generator with axial flux has been simulated. This motor/generator setup incorporates high voltage technology with the use of NdFeB permanent magnets and an air wound stator. The simulation topology used was partly chosen for simulation simplicity and can most likely be enhanced. The simulated motor/generator is intended for a flywheel storage system situated in e.g. a bus. However, this flywheel technology is scalable and larger machines can be constructed for the applications of e.g. stabilizing the electric grid.

Acknowledgements

Dr Karl Erik Karlsson and Dr Arne Wolfbrandt have given valuable support in implementing the FEM simulation. Eskilstuna Energi and Miljö and the Swedish Energy Agency (STEM), Swedish Defence Research Institute (FOI) and Swedish Defence Material Administration (FMV) are acknowledged for their financial support of this research project.

References

[1] Stodola A. Steam and gas turbines. New York: McGraw-Hill Book Company, Inc.; 1927.
[2] Bitterly JG. Flywheel technology: past, present, and 21st century projections. IEEE Aerospace Electron Syst Mag 1998;13:13–6.
[3] Vattenkraften i Sverige Royal Swedish Academy of Engineering Sciences, IVA; 2002.
[4] Leijon M, Dahlgren M, Walfridsson L, Li Ming, Jaksts A. A recent development in the electrical insulation system of generators and transformers. IEEE Electrical Insulation Mag 2001;17(3):10–5.
[5] Leijon, M. et al. Breaking conventions in electrical power plants, CIGRÉ paper; 1998, 11/37–03.
[6] Leijon M, Liu R. Energy technologies: electric power generators. vol. 3.: Landolt-Börnstein; 2002 (Inbook 4) p. 151–164.
[7] Leijon M, Berggren B, Owman F, Karlsson T. High voltage power generators without transformers. J Hydropower Dams 1998;37(4):40.
[8] Johansson SG, Larsson B. Short circuit tests on a high voltage, cable wound hydropower generator. IEEE Trans Energy Convers 2004;19(1):28–33.
[9] 1.5 kW Electromechanical battery system flywheel energy systems Inc. CETC-0100-01 Rev. 2.
[10] Gabrys CW. High Performance Composite Flywheel, US patent Pub. No.: US 2001/0054856 A1; 27 Dec 2001.

[11] MS-196. Project all electric vehicle (AEV). RTP 16.02 inom WEAG. Technical Report No. 1; Nov–Dec 2001.
[12] Taylor P, Johnsson L, Reichert K, DiPietro P, Philip J, Butler P. A summary of the state of the art of superconducting magnetic energy storage systems, flywheel energy storage systems and compressed air energy storage systems SAND99-1854, unlimited release. Albuquerque, New Mexico 87185 and Livermore, California 94550: Sandia National Laboratory; 1999.
[13] Fremery JK. Axially stabilized magnetic bearing having a permanently magnetized radial bearing, US patent nr 5,126,610; 30 Jun 1992.
[14] Swedish patent nr 508 442, Elektrodynamiskt magnetlager; 1998.
[15] Zhang Z, Profumo F, Tenconi A. Axial flux wheel machines for electric vehicles. Electr Machines Power Syst 1996;24:83–96.
[16] Platt D. Permanent magnet synchronous motor with axial flux geometry. IEEE Trans Magn 1989;25: 3076–9.
[17] Jensen CC, Profumo F, Lipo TA. A low-loss permanent-magnet brushless DC motor utilizing tape wound amorphous iron. IEEE Trans Ind Appl 1992;28:646–51.
[18] Sahin F, Vandenput AJA. Design considerations of the flywheel-mounted axial-flux permanent-magnet machine for a hybrid electric vehicle. Eighth European conference on power electronics and applications. EPE'99; Sept. 1999.
[19] Sahin F, Tuckey AM, Vandenput AJA. Design, development and testing of a high-speed axial-flux permanent-magnet machine Conference Record of the 2001 IEEE Industry Applications Conference, p. 1640–1647.
[20] Wijenayake AH, Bailey JM, McCleer PJ. Design optimization of an axial gap permanent magnet brushless DC motor for electric vehicle applications. IEEE Conf Record 1995 p. 685–692.
[21] Furlani EP. Computing the field in permanent-magnet axial-field motors. IEEE Trans Magn 1994;30(5):3660–3.
[22] Ojo O. Multiobjective optimum design of electrical machines for variable speed motor drives. IEEE Conf Record 1991 p. 163–168.
[23] Slemon GR. On the design of high performance PM motors. IEEE Conf Record 1992 p. 279–285.
[24] Hippner M, Harley RG. Looking for an optimal rotor for high speed permanent magnet synchronous machine. IEEE Conf Record 1992 p. 265–270.
[25] Jonson D, Pillay P, Malengret M. High speed PM motor with hybrid magnetic bearing for kinetic energy storage. Proc IEEE Ind Appl Soc 2001;1:57–63.
[26] Hull JR, Turner LR. Magnetomechanics of internal-dipole, Halbach-array motor/generators. IEEE Trans Magn 2000;36:2004–11.
[27] Kim WH, Kim JS, Baek JW, Ryoo HJ, Rim GH, Choi SK. Improving efficiency of flywheel energy storage system with a new system configuration PESC 98 Record. 29th Annual IEEE Power Electronics Specialists Conference; 1998, p. 24–28.
[28] Aanstoos TA, Kajs JP, Brinkman WG, Liu HP, Ouroua A, Hayes RJ, et al. High voltage stator for a flywheel energy storage system. IEEE Trans Magn 2001;37:242–7.
[29] Hofmann H, Sanders SR. Synchronous reluctance motor/alternator for flywheel energy storage systems. IEEE Power Electron Transport 1996;199–206.
[30] Powerex, Inc., homepage accessed Nov 2004, http://www.pwrx.com/.
[31] CT-Concept Technology Ltd, homepage accessed Nov 2004, http://www.igbt-driver.com/english/news/scale_hvi.shtml.
[32] Enjeti PN, Ziogas PD, Lindsay JF. Programmed PWM techniques to eliminate harmonics: a critical evaluation. IEEE Trans Ind Appl 1990;26:302–16.
[33] Cengelci E, Enjeti P. Modular PM generator/converter topologies, suitable for utility interface of wind/micro turbine and flywheel type electromechanical energy conversion systems. Conference Record of the 2000 IEEE Industry Applications Conference, vol. 4, p. 2269–2276.
[34] Mellor PH, Schofield N, Howe D. Flywheel and supercapacitor peak power buffer technologies, IEE seminar electric hybrid fuel cell vehicles, p. 8/1–5.
[35] Iglesias IJ, Garcia-Tabares L, Agudo A, Cruz I, Arribas L. Design and simulation of a stand-alone winddiesel generator with a flywheel energy storage system to supply the required active and reactive power. IEEE Conf Proc 2000;3:1381–6.
[36] Kan HP, Chau KT, Cheng M. Development of a doubly salient permanent magnet motor flywheel energy storage for building integrated photovoltaic system APEC 2001, Proceedings of the 16th IEEE conference, p. 314–320.

[37] Yoon-Ho K, Kyoung-Hun L, Young-Hyun C, Young-Keun H. Comparison of harmonic compensation based on wound/squirrel-cage rotor type induction motors with flywheel. Proceedings of third international conference on power electronics and motion control; 2000, p. 531–536.
[38] Jiancheng Z, Zhiye C, Lijun C, Yuhua Z. Flywheel energy storage system design for distribution network. IEEE Conf Proc 2000;4:2619–23.
[39] Reiner G, Wehlau N. Concept of a 50 MW/650 MJ power source based on industry-established MDS flywheel units. Twenty-eighth IEEE international conference on plasma science and 13th IEEE int. pulsed power conference; 2001, p. 248.
[40] Richard T, Belhomme R, Buchheit N, Gorgette F. Power quality improvement case study of the connection of four 1.6 MVA flywheel dynamic UPS systems to a medium voltage distribution network. IEEE/PES Transmission Distribution Conf Exposition 2001 p. 253–258.
[41] Truong LV, Wolff FJ, Dravid NV. Simulation of flywheel electrical system for aerospace applications. Collection of Technical Papers. 35th Intersociety Energy Conversion Engineering Conference and Exhibit (IECEC) (Cat. No. 00CH37022). vol. 1, pt. 1 2000 p. 601–68.
[42] Chalmers BJ. Developments in electrical machines using permanent magnets. J Magn Magn Mater 1996:131–2.
[43] Lorrain P, Corson DR. Electromagnetism principles and applications, 2nd ed. W.H. Freeman and Company; 1990.
[44] Http://www.euromag.se available online July 2004, from Euromag.
[45] Robert H, Joseph B, Alan W. Flywheel batteries come around again. IEEE Spectrum 2002 p. 46–51.
[46] Henderson Ellis CW, Stoffer JH. Kinetic energy storage system, US patent nr US 5,931,249; 3 Aug 1999.
[47] Bakholdin D, Bosley RW, Rosen HA, Pearson CC, Pano SB. Hub and cylinder design for flywheel for mobile energy storage US Patent No: 6,175,172 B1; 16 Jan 2001.
[48] Sung TH, Lee JS, Han YH, Han SC, Kim CJ, Hong GW, et al. Flywheel energy storage system with a horizontal axle mounted on high Tc superconductor bearings. Cryogenics 2001;41:461–7.
[49] Gupta R, Yoshino T, Salito Y. Finite element solution of permanent magnetic field. IEEE Trans Magn 1990;26(2):383–6.